Article:
Stairs, B., Johnson, H., Mondron, K. et al. (2026) Genomic analyses of globally distributed Rhizopus microsporus populations indicate clinical isolates derived from environmental diversity reservoirs. Mycologia. ISSN: 0027-5514

https://doi.org/10.1080/00275514.2025.2594974

MYCOLOGIA

Mycologia

ISSN: 0027-5514 (Print) 1557-2536 (Online) Journal homepage: www.tandfonline.com/journals/umyc20

Genomic analyses of globally distributed *Rhizopus microsporus* populations indicate clinical isolates derived from environmental diversity reservoirs

Brandon Stairs, Hayden Johnson, Kyle Mondron, Kimberly C. Syring, Andreas Guerrero, Elizabeth R. Ballou, Jason S. King, Teresa E. Pawlowska, Rasheed Adeleke, David A. Stevens & Jessie K. Uehling

To cite this article: Brandon Stairs, Hayden Johnson, Kyle Mondron, Kimberly C. Syring, Andreas Guerrero, Elizabeth R. Ballou, Jason S. King, Teresa E. Pawlowska, Rasheed Adeleke, David A. Stevens & Jessie K. Uehling (28 Jan 2026): Genomic analyses of globally distributed *Rhizopus microsporus* populations indicate clinical isolates derived from environmental diversity reservoirs, Mycologia, DOI: 10.1080/00275514.2025.2594974

To link to this article: https://doi.org/10.1080/00275514.2025.2594974

MYCOLOGIA
https://doi.org/10.1080/00275514.2025.2594974

Taylor & Francis
Taylor & Francis Group

Genomic analyses of globally distributed *Rhizopus microsporus* populations indicate clinical isolates derived from environmental diversity reservoirs

Brandon Stairs[a], Hayden Johnson[a], Kyle Mondron[a], Kimberly C. Syring[a], Andreas Guerrero[a], Elizabeth R. Ballou[b], Jason S. King[c], Teresa E. Pawlowska[d], Rasheed Adeleke[e], David A. Stevens[f], and Jessie K. Uehling[a]

[a]Department of Botany and Plant Pathology, Oregon State University, 2701 NW Orchard Ave, Corvallis, Oregon 97331, USA; [b]MRC Centre for Medical Mycology, University of Exeter, Geoffrey Pope Building, Stocker Road, Exeter EX4 4QD, UK; [c]School of Biosciences, University of Sheffield, Alfred Denny Building, Western Bank S10 2TN, UK; [d]School of Integrative Plant Science, Cornell University, 334 Plant Science, Ithaca, New York 14853-5904, USA; [e]Unit for Environmental Sciences and Management, North-West University, 12 Thabo Mbeki Rd, Private Bag X6001, Potchefstroom 2520, South Africa; [f]Division of Infectious Diseases and Geographic Medicine, Stanford University Medical School, 19070 Portos Dr, Stanford, California 94305, USA

ABSTRACT

Mucormycosis is a group of diseases that is increasing in frequency. A common opportunistic human fungal pathogen in this group is *Rhizopus microsporus*, which is a globally distributed species present in soil-associated environments. A subset of isolates in this species host endobacteria that are hypothesized to influence fungal pathogenicity in both clinical and environmental settings. We have limited understanding of how clinically and environmentally derived isolates are related or how physiological attributes, including thermotolerance and endosymbiosis, are correlated with population structure. Traditional molecular barcodes used to assess intraspecific relationships, such as ribosomal DNA internal transcribed spacer (ITS-rDNA)–based markers, do not provide species-level resolution, necessitating analyses of whole genome data. In this study, we generated novel whole genome sequencing data for six *R. microsporus* isolates and combined these data with publicly available whole genome sequences of 46 *R. microsporus* isolates. We evaluated these sequences to understand the evolutionary relationships among clinical and environmental isolates using phylogenomic and single nucleotide polymorphism (SNP)-based population genomics methods. We further studied their relationships by quantifying and comparing potential physiological differences and endosymbiont presence in a subset of 16 isolates with live cultures. We found that clinical isolates that originate from environmental settings contain higher molecular diversity than subpopulations isolated from clinical settings. We observed that environmental isolates grow faster than clinical isolates at temperatures between 22 and 37 C and that 7 of 16 (44%) contain endobacteria in the genus *Mycetohabitans* (Burkholderiales). Lastly, we observed that genome assembly size in *R. microsporus* is variable and that long-read sequencing technologies greatly enhance our ability to investigate the underlying genomic features. Our study provides a valuable backdrop for probing the basic biology and applied biomedical importance of *Rhizopus* and related fungi that cause mucormycosis.

ARTICLE HISTORY
Received 27 February 2025
Accepted 31 October 2025

KEYWORDS
Endosymbiont; evolution; mucormycosis; phylogenomics; populations; *Rhizopus*

INTRODUCTION

Rhizopus microsporus (Mucorales, Mucoromycota) is a globally distributed fungal species that causes infections of plants and animals with major implications for agriculture and medicine (Lackner et al. 2009; Jeong et al. 2019; Prakash and Chakrabarti 2019, 2021; Prakash et al. 2020). The relevance of *R. microsporus* has been highlighted by the recent increased prevalence of mucormycosis, a disease caused by *R. microsporus* and related fungi that generally impacts immunocompromised individuals (Spellberg et al. 2009; Ibrahim et al. 2012; Jeong et al. 2019; Prakash and Chakrabarti 2019). Study of the evolutionary history in this group has been complicated by a complex taxonomic history, which is partially based on very subtle differences in micromorphology. This has led to multiple, sometimes conflicting descriptions of species and varieties (Schipper and Stalpers 1984; Zheng et al. 2007; Corzo-León et al. 2018). However, it is unclear whether such distinctions reflect evolutionary processes or pathogenic potential that could be inferred by constructing DNA sequence–based genealogies. Further, the traditionally used molecular barcodes, such as ribosomal DNA

CONTACT Jessie K. Uehling jessie.uehling@oregonstate.edu
Supplemental data for this article can be accessed online at https://doi.org/10.1080/00275514.2025.2594974

Published online 28 Jan 2026

internal transcribed spacer (ITS-rDNA) barcode sequencing, do not provide accurate species-level resolution in this fungal group (Kontoyiannis and Lewis 2011; Millon et al. 2013; Skiada et al. 2018). Therefore, phylogenetic and population analyses of whole genome sequencing data are necessary to better understand the diversity and evolutionary history of *R. microsporus*.

Rhizopus microsporus isolates have been demonstrated to host endosymbiotic bacteria often related to the genus *Burkholderia* and other Proteobacteria (Partida-Martinez et al. 2007; Lackner and Hertweck 2011) that may facilitate fungal virulence via manipulation of phagocyte behavior (Itabangi et al. 2022). These endosymbionts, including *Mycetohabitans* species, produce secondary metabolites used to evade predators and decay tissues (Partida-Martinez and Hertweck 2005; Partida-Martinez et al. 2007; Lackner and Hertweck 2011; Lackner et al. 2011; Richter et al. 2024). However, *R. microsporus* fungi do not consistently host endobacteria, and much remains to be learned regarding endosymbiotic taxonomic identity, interaction mechanisms between endosymbionts and their host fungi, and the ubiquity of endosymbiont functional genomic content (Partida-Martinez et al. 2007; Robinson et al. 2021; Itabangi et al. 2022; Uehling et al. 2023; Carpenter et al. 2024). Better understanding of endosymbiont ubiquity, abundance, and diversity is necessary to evaluate their influence on fungal physiology, including virulence.

The increasingly frequent mucormycosis infection rates, especially associated with the outbreaks during the COVID-19 pandemic, underscore the need to evaluate sources and infection mechanisms of clinical *R. microsporus* isolates (Antoniadou 2009; Cheng et al. 2009; Pandey et al. 2018). Some *R. microsporus* isolates are able to grow at human body temperature, which is hypothesized to contribute to pathogenicity (Peixoto et al. 2003; Dolatabadi et al. 2014; Kaerger et al. 2015). However, environmental isolates live in locations where temperatures regularly dip below freezing (0 C) and are isolated from diverse clinical, environmental, and food products, suggesting the existence of subpopulations with variable physiologies and temperature tolerances (Verweij et al. 1997; Zheng et al. 2007; Cheng et al. 2009; Dolatabadi et al. 2014; Bowers et al. 2020; Prakash et al. 2020; Cabrera-Rangel et al. 2022).

In this study, we provide an account of genetic and phenotypic diversity across 61 Mucorales isolates, including 52 *R. microsporus* isolates from clinical and environmental settings, using whole genome sequence data in a phylogenomic and population structure framework. To quantify potential phenotypic differences between clinical and environmental isolates, we measured radial mycelial growth rates in a subset of our isolate collection at human body temperature (37 C) and room temperature (22 C). In addition, we explore the presence and phylogenetic relationships between *Rhizopus* hosts and their endosymbiotic bacteria, which may play a critical role in host virulence. This research serves as a foundation for future studies of *R. microsporus* and the molecular mechanisms that underpin its roles in the clinical and environmental settings.

MATERIALS AND METHODS

Taxon sampling and culture conditions.—Data for the analyses described here were obtained through a combination of novel whole genome sequencing and reanalysis of publicly available data from isolates obtained in both clinical and environmental global sources (FIG. 1, TABLE 1). We obtained raw, short-read (Illumina, San Diego, CA) sequencing data from 46 previously sequenced and accessioned *R. microsporus* isolates from the National Center for Biotechnology Information (NCBI) Sequence Read Archive (SRA) and GenBank (TABLE 1). We combined these data with novel Illumina genome sequence data from cultures of six isolates (CBS 112285, CBS 11563, ATCC 52812, ATCC 56028, ATCC 56019, and NRRL 5549). We also sequenced the following isolates: ATCC 62417, ATCC 52814, and NRRL 5546 with Nanopore sequencing technologies (TABLE 1). All physiological experiments were performed at Oregon State University (OSU) in a BSL-2 (Biosafety Level 2) laboratory certified by the OSU Institutional Biosafety Committee under Proposal 2524.

DNA extractions and Illumina genome sequencing.—Fungal cultures were maintained on 2% malt extract agar (Difco, Franklin Lakes, New Jersey) on agar slants and in 60 mm × 15 mm Petri dishes sealed with Parafilm and stored at room temperature. DNA was extracted and analyzed for Illumina sequencing as previously described (Uehling et al. 2017). Briefly, hyphae were grown in malt extract broth (Difco) in a shaking incubator (Infors HT, Basel, Switzerland) at 120 revolutions per minute (rpm) at 22 C for 7 days and collected using a vacuum pump with sterilized Miracloth (Millipore, Burlington, Massachusetts). Fungal tissues were then homogenized in cetyltrimethylammonium bromide (CTAB) extraction buffer amended with proteinase K (VWR, Radnor, Pennsylvania). After incubating at 65 C for 60 min, a phase separation step was conducted twice with a 24:1 mixture of chloroform:isoamyl alcohol (Sigma-

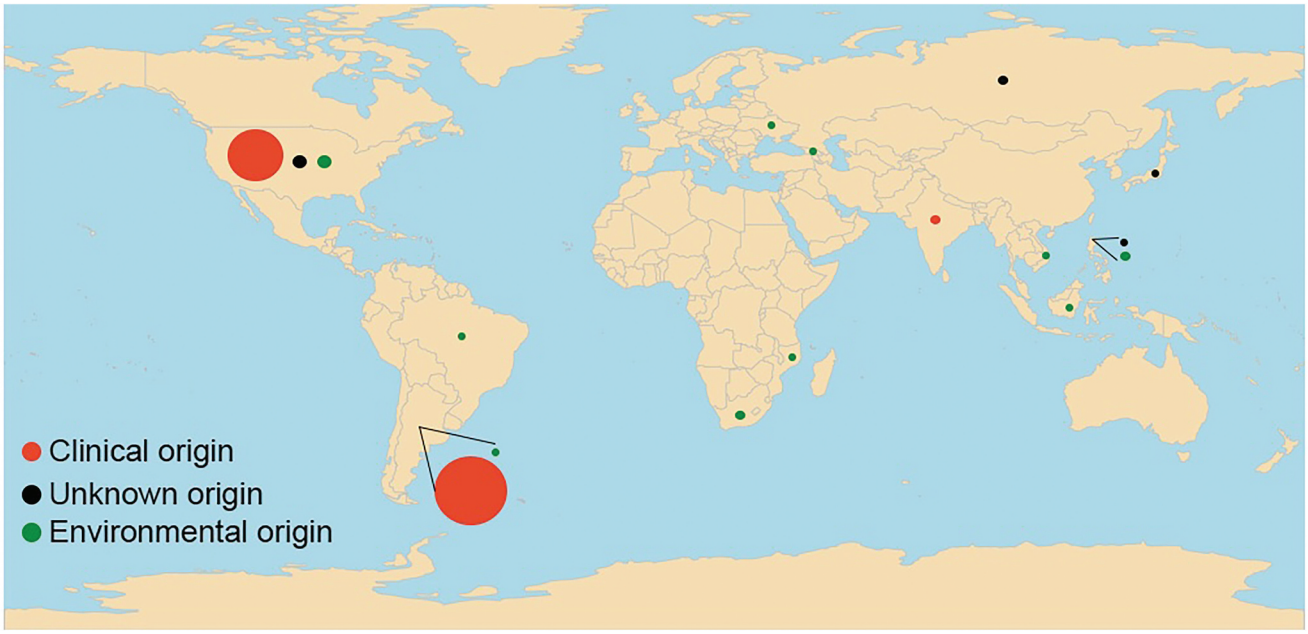

Figure 1. Isolate origin for genome data of *R. microsporus* analyzed. Isolation sources are indicated by circle color as follows: clinical (red), environmental (green), and unknown (black). Circle sizes reflect the number of isolates from each location in accordance with TABLE 1.

Aldrich, St. Louis MO) before DNA was precipitated with isopropanol (VWR). DNA pellets were washed with 70% ethanol, dried overnight, resuspended in nuclease-free water, qualified using a NanoDrop One (Thermo Scientific, Waltham, Massachusetts), and quantified with a Broad Range double-stranded Qubit assay on a Qubit 2.0 fluorometer (Qubit, Waltham, Massachusetts). Before sequencing, DNA samples were purified using a genomic DNA Clean & Concentrator kit (Zymo Research, Irvine, California), and DNA quantity and quality were reassessed with Qubit. For Illumina genomes, 2 × 150 paired-end reads were generated on an Illumina HiSeq system (San Diego, California) at the Genomics and Cell Characterization Core Facility at the University of Oregon (Eugene, Oregon) at a read depth of ~50× coverage (TABLE 1).

Nanopore genome sequencing.—For Nanopore genome sequencing, three isolates of *Rhizopus microsporus* (ATCC 62417, ATCC 52814, and NRRL 5546) were selected because they represent fungal diversity across the environmental clade, they host diverse endobacteria, and they have a wide range of estimated genome assembly sizes. For each isolate, fungal biomass was split into five tubes, and DNA was isolated using the extraction protocol described above. After extraction, samples were checked via NanoDrop and Qubit for quality and concentration, and replicate samples were pooled for each isolate before being cleaned and concentrated using a genomic DNA Clean & Concentrator kit (Zymo Research). Samples were assessed again for quality using a Qubit 2.0 fluorometer. Samples with NanoDrop 260/280 ratio values of ~1.8–2.0 and 260/230 ratio values of ~2.0–2.2 were used as quality cutoffs. Two micrograms of high-molecular-weight DNA from each sample was used for size selection and library preparation. Next, samples were prepared using a Ligation Sequencing Kit V14 (Oxford Nanopore Technologies, Oxford, UK) following the protocol provided by the manufacturer. Samples were sequenced on a MinION flow cell (Oxford Nanopore Technologies) and were run sequentially with a wash with a Flow Cell Wash Kit (Oxford Nanopore Technologies) between runs. This resulted in 2.8–6.7 GB of data, or ~56–134× coverage per isolate for downstream analyses (TABLE 1).

PCR amplification and gene sequencing.—Polymerase chain reaction (PCR) amplification of rDNA genes for species/taxon identification was performed using GoTaq Flexi polymerase (Promega, Madison, Wisconsin) as previously published (Uehling et al. 2017). The following primer pairs were used to amplify the fungal internal transcribed spacer (ITS) and bacterial endosymbiont 16S genes, respectively: forward primer ITS1F/reverse primer ITS4R and forward primer 8 F/reverse primer 1492 R (White et al. 1990; Reysenbach et al. 1992; Baker et al. 2003). PCR

Table 1. Mucorales isolates used in genomic analyses.

Isolate[a,b]	Species	Illumina genome size (Mb)	Nanopore genome size (Mb)	Isolation source	Geography	Thermotolerance assessed	GenBank
16-129	*R. microsporus*	NA	NA	Clinical	USA	Yes	NA
16-88	*R. microsporus*	NA	NA	Clinical	USA	Yes	NA
17-102	*R. microsporus*	NA	NA	Clinical	USA	Yes	NA
21-01	*R. microsporus*	NA	NA	Clinical	USA	Yes	NA
460-P-21	*R. microsporus*	23.5	NA	Clinical	India	No	PRJNA931319
415-P-21	*R. microsporus*	25.2	NA	Clinical	India	No	PRJNA931319
ATCC 11559	*R. microsporus* var. *chinensis*	24.7	NA	Unknown	Russia	No	PRJNA330885
ATCC 52812	***R. microsporus* var. *chinensis***	**28.5**	**NA**	Unknown	**USA**	**Yes**	**PRJNA942854**
ATCC 52813	*R. microsporus* var. *microsporus*	26	NA	Soil, environmental	Ukraine	Yes	PRJNA205957
***ATCC 52814**	***R. microsporus* var. *microsporus***	**25.3**	**40.3**	**Soil, environmental**	**Republic of Georgia**	**Yes**	**PRJNA330886 / PRJNA1282220**
ATCC 56019	***R. microsporus***	**28.8**	**NA**	**Unknown**	**Unknown**	**Yes**	**PRJNA942854**
***ATCC 62417**	***R. microsporus***	**42.6**	**59.9**	**Unknown**	**Japan**	**Yes**	**PRJEB7410 / PRJNA1282204**
B07367	*R. microsporus* var. *microsporus*	24.4	NA	Unknown	USA	No	PRJ A526061
B06600	*R. microsporus* var. *oligosporus*	45.4	NA	Clinical	USA	No	PRJ A526061
B06590	*R. microsporus* var. *oligosporus*	44.1	NA	Clinical	USA	No	PRJ A526061
B05459	*R. microsporus* var. *rhizopodiformis*	24.4	NA	Clinical	USA	No	PRJ A526061
B07675	*R. microsporus* var. *rhizopodiformis*	24.4	NA	Chest tissue, clinical	USA	No	PRJ A526061
B07643	*R. microsporus* var. *rhizopodiformis*	24.4	NA	Clinical	USA	No	PRJ A526061
B07585	*R. microsporus* var. *microsporus*	28.5	NA	Clinical	USA	No	PRJ A526061
B07386	*R. microsporus* var. *microsporus*	29.7	NA	Skin, clinical	USA	No	PRJ A526061
B10187	*R. microsporus* var. *rhizopodiformis*	24.4	NA	Wound, clinical	USA	No	PRJ A526061
B08956	*R. microsporus* var. *microsporus*	28	NA	Respiratory, clinical	USA	No	PRJ A526061
B11541	*R. microsporus* var. *microsporus*	49.8	NA	Clinical	Argentina	No	PRJ A526061
B11543	*R. microsporus* var. *rhizopodiformis*	24.4	NA	Femur, clinical	Argentina	No	PRJ A526061
B11547	*R. microsporus* var. *rhizopodiformis*	24.4	NA	Femur, clinical	Argentina	No	PRJ A526061
B11535	*R. microsporus* var. *rhizopodiformis*	24.4	NA	Clinical	Argentina	No	PRJ A526061
B11553	*R. microsporus* var. *rhizopodiformis*	24.4	NA	Knee, clinical	Argentina	No	PRJNA526061
B11550	*R. microsporus* var. *rhizopodiformis*	24.4	NA	Knee, clinical	Argentina	No	PRJ A526061
B11554	*R. microsporus* var. *rhizopodiformis*	44.6	NA	Bone, clinical	Argentina	No	PRJ A526061
B11549	*R. microsporus* var. *rhizopodiformis*	24.4	NA	Environmental	Argentina	No	PRJ A526061
B10548	*R. microsporus* var. *rhizopodiformis*	24.4	NA	Clinical	USA	No	PRJ A526061
B11523	*R. microsporus* var. *rhizopodiformis*	24.4	NA	Sternum muscle, clinical	Argentina	No	PRJ A526061
B11147	*R. microsporus* var. *rhizopodiformis*	24.4	NA	Clinical	USA	No	PRJNA526061
B11532	*R. microsporus* var. *rhizopodiformis*	24.4	NA	Abdominal fluid, clinical	Argentina	No	PRJ A526061
B11531	*R. microsporus* var. *rhizopodiformis*	24.4	NA	Bone, clinical	Argentina	No	PRJ A526061
B11533	*R. microsporus* var. *rhizopodiformis*	25.1	NA	Abdominal, clinical	Argentina	No	PRJ A526061
B11552	*R. microsporus* var. *rhizopodiformis*	24.4	NA	Clinical	Argentina	No	PRJ A526061
B11557	*R. microsporus* var. *microsporus*	42.7	NA	Renal tissue, clinical	Argentina	No	PRJ A526061
B11556	*R. microsporus* var. *rhizopodiformis*	24.4	NA	Knee, clinical	Argentina	No	PRJ A526061
B11555	*R. microsporus* var. *rhizopodiformis*	25.1	NA	Pericardial fluid, clinical	Argentina	No	PRJ A526061
CBS 112285	***R. microsporus* var. *microsporus***	**29.1**	**NA**	**Ground nuts, environmental**	**Mozambique**	**Yes**	**PRJNA942854**
CBS 11563	***R. microsporus* var. *microsporus***	**28.5**	**NA**	**Sufu starter, environmental**	**Vietnam**	**Yes**	**PRJNA942854**
CBS 344.29	*R. microsporus*	31.6	NA	Unknown	Russia	No	PRWEB 7409
CBS 357.93	*R. microsporus* var. *azygosporus*	36.7	NA	Tempeh, environmental	Indonesia	No	PRJNA418064
GL-19	*R. microsporus* var. *microsporus*	35.5	NA	Environmental	USA	No	PRJNA475137
NRRL 13129	*R. microsporus*	28.5	NA	Unknown	Africa	No	PRJNA536200
***NRRL 5546**	***R. microsporus***	**27.7**	**24.9**	**Soil, environmental**	**Brazil**	**Yes**	**PRJNA537141 / PRJNA1282205**
NRRL 5547	*R. microsporus*	28.8	NA	Soil, environmental	Philippines	Yes	PRJNA537142
NRRL 5548	*R. microsporus*	27.9	NA	Soil, environmental	Philippines	Yes	PRJNA537143

(*Continued*)

Table 1. (Continued).

Isolate[a,b]	Species	Illumina genome size (Mb)	Nanopore genome size (Mb)	Isolation source	Geography	Thermotolerance assessed	GenBank
NRRL 5549	***R. microsporus***	**27.8**	**NA**	**Rabbit dung, environmental**	**USA**	**Yes**	**PRJNA942854**
NRRL 5550	*R. microsporus*	27.7	NA	Unknown	USA	No	PRJNA537144
NRRL 5551	*R. microsporus*	29.6	NA	Unknown	Philippines	No	PRJNA535095
NRRL 5552	*R. microsporus*	27.7	NA	Creek sediment, environmental	USA	No	PRJNA535096
NRRL 5553	*R. microsporus*	28.8	NA	Soil, environmental	South Africa	No	PRJNA537145
NRRL 5558	*R. microsporus*	27.9	NA	Corn, environmental	Unknown	No	PRJNA535003
P3-GL61	*R. microsporus*	24.4	NA	Clinical	USA	No	PRJNA475137
XY03801	*R. microsporus*	29.3	NA	Soil, environmental	South Africa	No	PRJNA765118
RA 99-880	*R. arrhizus*	42	NA	Clinical	USA	No	PRJNA680572
ATCC 56028	***R. arrhizus***	**37.6**	**NA**	Unknown	Unknown	Yes	**PRJNA942854**
B7407	*R. arrhizus*	37.8	NA	Clinical	USA	No	PRJNA184879
NRRL 13440	*R. arrhizus*	36.7	NA	Clinical	USA	No	PRJNA186013
NRRL 5554	*R. arrhizus*	38.3	NA	Soil, environmental	South Africa	No	PRJNA537146
NRRL A-17693	*Circinella* spp.	44.9	NA	Unknown	Unknown	No	PRJNA536201
NRRL 2417	*Circinella umbellata*	44.8	NA	Unknown	Unknown	No	PRJNA676535
NRRL 2628	*Circinella angarensis*	42.4	NA	Unknown	Unknown	No	PRJNA676550
B8987	*Mucor circinelloides*	32.6	NA	Clinical	USA	No	PRJNA184880

[a]Bold indicates isolates with genome sequences generated in this project using Illumina short-read sequencing technology.
[b]Asterisks indicate isolates with genome sequences generated in this project using Nanopore sequencing technology.

amplicons were visualized via gel electrophoresis using GelRed staining (Biotium, Fremont, California) on a 1% agarose gel and viewed using a Gel Imager (Azure Systems, Hayward, California). PCR products were purified using the ExoSAP-IT protocol (Thermo Fisher Scientific, Waltham, Massachusetts), sequencing was performed on an ABI 3730 capillary sequencing machine by the Center for Quantitative Life Sciences at Oregon State University (Corvallis, Oregon), and DNA sequences were analyzed using Sequencher 4.0 (Gene Codes, Ann Arbor, Michigan).

Whole genome assembly, annotation, and phylogenomic construction.—For the short-read, whole genome sequences included in this study, raw data were first treated using fastp 0.32.2 to trim Illumina TruSeq adapters and FastQC 0.11.9 to remove reads with a Phred score less than 15 (Chen et al. 2018). Illumina paired-end reads were de novo assembled using SPAdes 3.15.3, and contigs less than 500 base pairs in length were removed (Bankevich et al. 2012). Funannotate 1.8.14 was used to remove duplicate contigs, mask repetitive contig regions, and perform genome annotation with the BUSCO "Mucorales" database as gene evidence (Palmer and Stajich 2020). The Mucorales database was utilized in HMMER 3.32 to search for genes with an e-value cutoff of $1e^{-5}$, and the remaining protein sequences were aligned to the corresponding HMM profile (Eddy 1996, 2011). To perform multiple sequence alignment, trimAl 1.4 implemented a heuristic algorithm to align the protein sequences found in all taxa based on gap location and sequence similarity (Capella-Gutiérrez et al. 2009). The protein sequence alignments of each fungal taxon were concatenated together prior to phylogenomic construction (Amses et al. 2019). To determine the best substitution model, ModelFinder was performed and implemented through IQ-TREE 2.2.0 (Nguyen et al. 2015). Maximum-likelihood analysis was implemented using IQ-TREE with 100 bootstrap replicates, and the resulting data were plotted in R 4.1.2 (https://www.r-project.org) with *Mucor circinelloides* as an outgroup (Kalyaanamoorthy et al. 2017; Minh et al. 2020). Genome assembly sizes (TABLE 1) were determined using the following workflow. Raw data were filtered for quality using NanoFilt 2.8.0 with flags for Phred <7 and length <100 and assembled with Flye 2.9.4 using the meta flag and an overlap parameter of 1000 or larger (De Coster et al. 2018; Kolmogorov et al. 2019). Endosymbionts were removed from initial assemblies by binning contigs using MetaBAT2 2.17

and using nucleotide BLAST to distinguish between fungal and bacterial bins. The resulting assemblies were polished with Racon 1.4.20 followed by Medaka 2.0.1 (Medaka: Sequence correction provided by ONT Research, https://github.com/rrwick/Unicycler, accessed Feb 2025), and the final assembly was evaluated for quality using QUAST 5.2.0 (Vaser et al. 2017; Kang et al. 2019). Alignments are available in Supplementary Material.

Single nucleotide polymorphism analyses.—We evaluated the molecular divergence of fungal populations by analyzing single nucleotide polymorphisms (SNPs) from the genomes of each isolate. Raw reads were aligned to a reference genome for *Rhizopus microsporus* isolate B11533 using the Burrows-Wheeler Aligner (BWA) package (Li 2013). Assemblies were indexed, sorted, and converted to BAM format using SAMtools 1.17 (Li et al. 2009; Danecek et al. 2021). For a population analyses, BCFtools 1.9 was utilized to identify SNPs between each new assembly and the reference genome (Li 2011). Upon detecting a SNP, the corresponding locus was retained across all taxa. A minimum alignment read depth threshold of 200 was applied, filtering out low-quality SNPs. The data set was further refined to include only biallelic SNPs present across all taxa at a single locus. For each taxon, the retained SNPs were concatenated into a single genetic sequence, which was subsequently used for analyses. The maximum-likelihood analysis was performed with IQ-TREE 1.6.9 with 100 bootstrap replicates. To accurately compute the SNP data, an ascertainment bias correction was implemented to account for the removal of invariant loci in conjunction with the general time reversible model. The resulting phylogenetic tree was plotted using GGTREE in R 4.1.2 (https://www.r-project.org) with *M. circinelloides* as the outgroup (Nguyen et al. 2015).

We identified subpopulations by evaluating SNP diversity and isolation source for each isolate. SNPs were then curated and censored utilizing PLINK 1.9 (Purcell et al. 2007) to remove variants with a minor allele frequency lower than 3% or missing call frequencies greater than 15%. A comparison of the SNPs identified between *R. microsporus* isolates was performed using a principal component analysis (PCA) implemented with the R package ADEGENET 2.1.8 (Jombart 2008). Genetic admixture between *R. microsporus* populations was determined using ADMIXTURE 1.3.0 for K values 1–8. A cross-validation error estimate was performed using ADMIXTURE 1.3.0 to identify the most likely number of subpopulations or K value given the genomic data set (Alexander et al. 2009). The resulting data were plotted in R 4.1.2.

Thermotolerance analyses.—We quantified radial mycelial growth rates of 15 *R. microsporus* isolates (11 environmental and 4 clinical; TABLE 1) at varying temperatures on agar plates. For each isolate, three technical replicates were grown at 22 and 37 C in a randomized design with three technical replicates (TABLE 1). Isolates were cultured by placing 6-mm-diameter plugs onto the center of 100 mm × 15 mm Petri dishes containing 2% malt extract agar (Difco). To measure hyphal growth, the circumference of the outer hyphal ring was traced every 12 h until reaching the edge of the Petri dish. The dish was divided into quadrants, and in each quadrant the radius of hyphal growth was measured in mm from the center to the edge of each ring, resulting in four measurements for each time step. The radial mycelial growth rate (mm/day) was determined for each measurement, and the mean growth rate was calculated for each technical replicate. For each isolate at each temperature, the final mean growth rate was obtained by calculating the mean across the three technical replicates. The significance of differences between the isolation sources and temperature mean values was determined by two-way analysis of variance (ANOVA) with significance testing at $\alpha = 0.05$. The resulting data were analyzed and plotted in R 4.1.2.

RESULTS

Clinical isolates originate from environmental diversity reservoirs.—We performed phylogenomic analyses of 2385 single-copy orthologous genes (FIG. 2) and a whole genome data set of 3 932 827 loci containing SNPs to evaluate the evolutionary history of *Rhizopus* isolates. In our analyses, we detected *Rhizopus* species, *R. microsporus* and *R. arrhizus*, with bootstrap support of 100% on all major nodes (FIGS. 2 and 3) and forming a monophyletic clade sister to a *Circinella* clade (FIG. 2). We found a terminal clade composed largely of clinical *R. microsporus* var. *rhizopodiformis* isolates with origins spanning North and South America (FIGS. 1–3). Three misannotated isolates previously taxonomically classified as *R. microsporus* in the ATCC and NRRL culture databases were identified by our studies. Isolates ATCC 56028 and NRRL 5554 form a well-supported, monophyletic clade with *R. arrhizus* isolates (FIGS. 2 and 3), whereas NRRL A-17693 is taxonomically grouped with *Circinella* spp. (FIGS. 2 and 3).

We further utilized the results of our *Rhizopus* phylogenomic analyses to evaluate the diversity and relatedness of regional subpopulations and isolates from the environment compared with clinical sources. The results of our gene- and SNP-based analyses

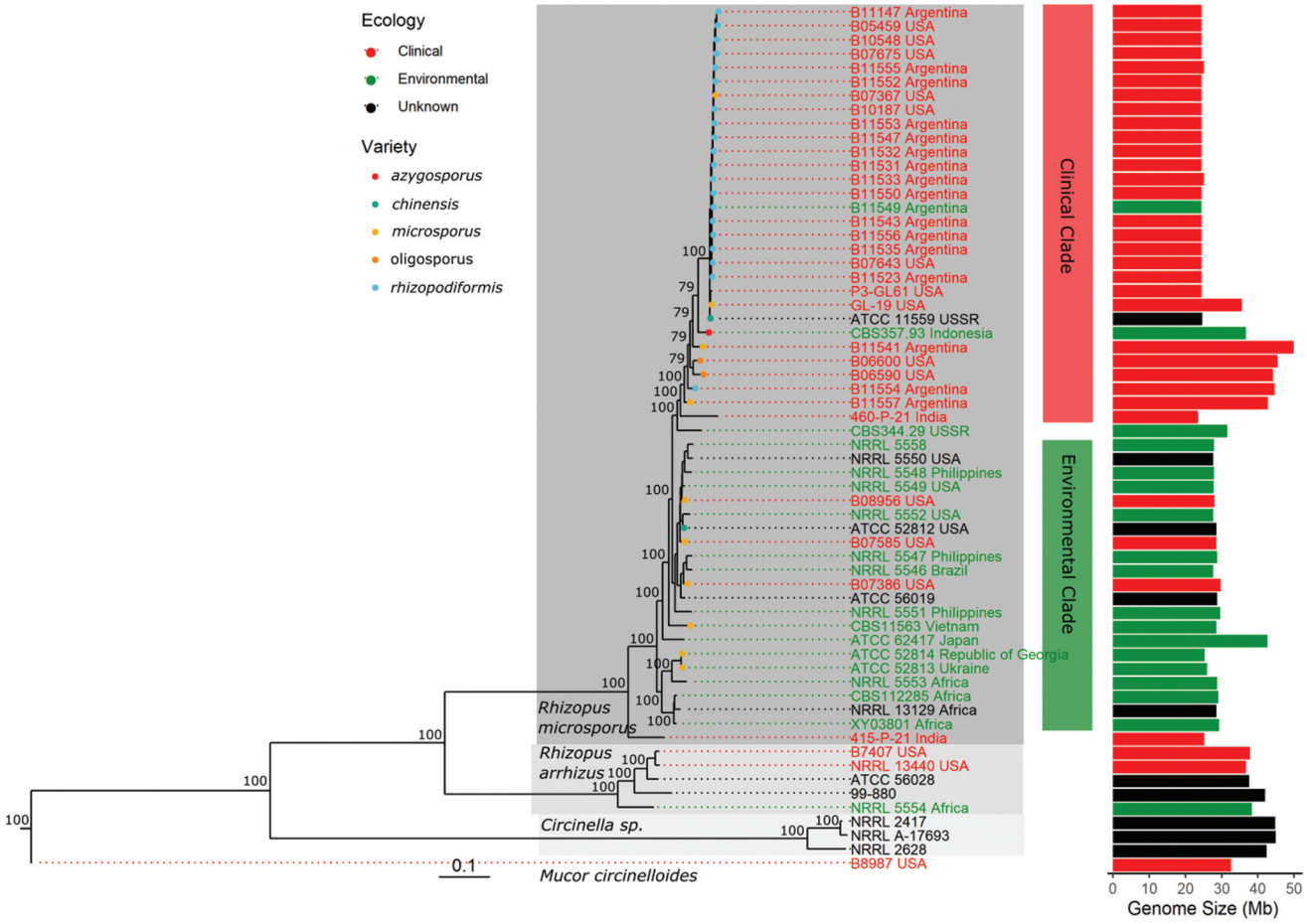

Figure 2. Maximum-likelihood phylogenomic tree. Phylogeny constructed using orthologous protein sequences. Orthologous protein sequences were obtained from the Mucorales genera *Rhizopus, Circinella*, and *Mucor*. Bootstrap support values are reported at each node. Isolation source is indicated by taxon coloring at branch tips as follows: clinical (red), environmental (green), and unknown (Black). The *R. microsporus* varieties *azygosporus, chinensis, rhizopodiformis, oligosporus*, and *microsporus* are represented by branch tips colored red, green, turquoise, orange, and yellow, respectively.

suggest that isolates group into two clades with few exceptions: one paraphyletic, basal clade of largely environmental isolates and a more derived clade of mostly clinical isolates that are less diverse and more closely related to each other (FIGS. 2 and 3). We refer to these groups as clinical and environmental clades, respectively.

In the environmental clade, we found isolates from diverse geographic locations, including the USA, Brazil, the Philippines, Vietnam, Japan, the Republic of Georgia, Africa, India, and Ukraine (FIGS. 1–3). Interspersed in this clade are five clinical isolates: B08956 (USA), B07585 (USA), B07386 (USA), 460-P-21 (India), and 415-P-21 (India). In contrast, in the clinical clade, all but four isolates were isolated from clinical settings in the USA and Argentina. Isolates CBS 344.29 (USSR), CBS 357.39 (Indonesia), ATCC 11559 (USSR), and B11549 (Argentina) were grouped in the clinical clade but were of environmental or unknown origin (FIGS. 2 and 3).

All clinical isolates from Argentina and those from several other locations included in this analysis grouped phylogenetically in the clinical clade with very few molecular differences, indicating clonality (FIGS. 2 and 3). In the environmental clade, the longer branch lengths observed suggest greater molecular diversity and larger effective population sizes (FIGS. 2 and 3). Together, these results indicate that the environment harbors a pool of molecular diversity and that a subset of these isolates go on to infect patients in clinics, leading to clonal lineages.

We evaluated the population structure of whole genome SNP data to better understand population diversity of *R. microsporus* using the program ADMIXTURE. Cross-validation error analysis for the ideal number of subpopulations in ADMIXTURE resulted in K = 8, indicating there are most likely 8 subpopulations represented (FIG. 4). We then utilized a principal component analysis to further visualize the SNP diversity within and between subpopulations. The results further underscore

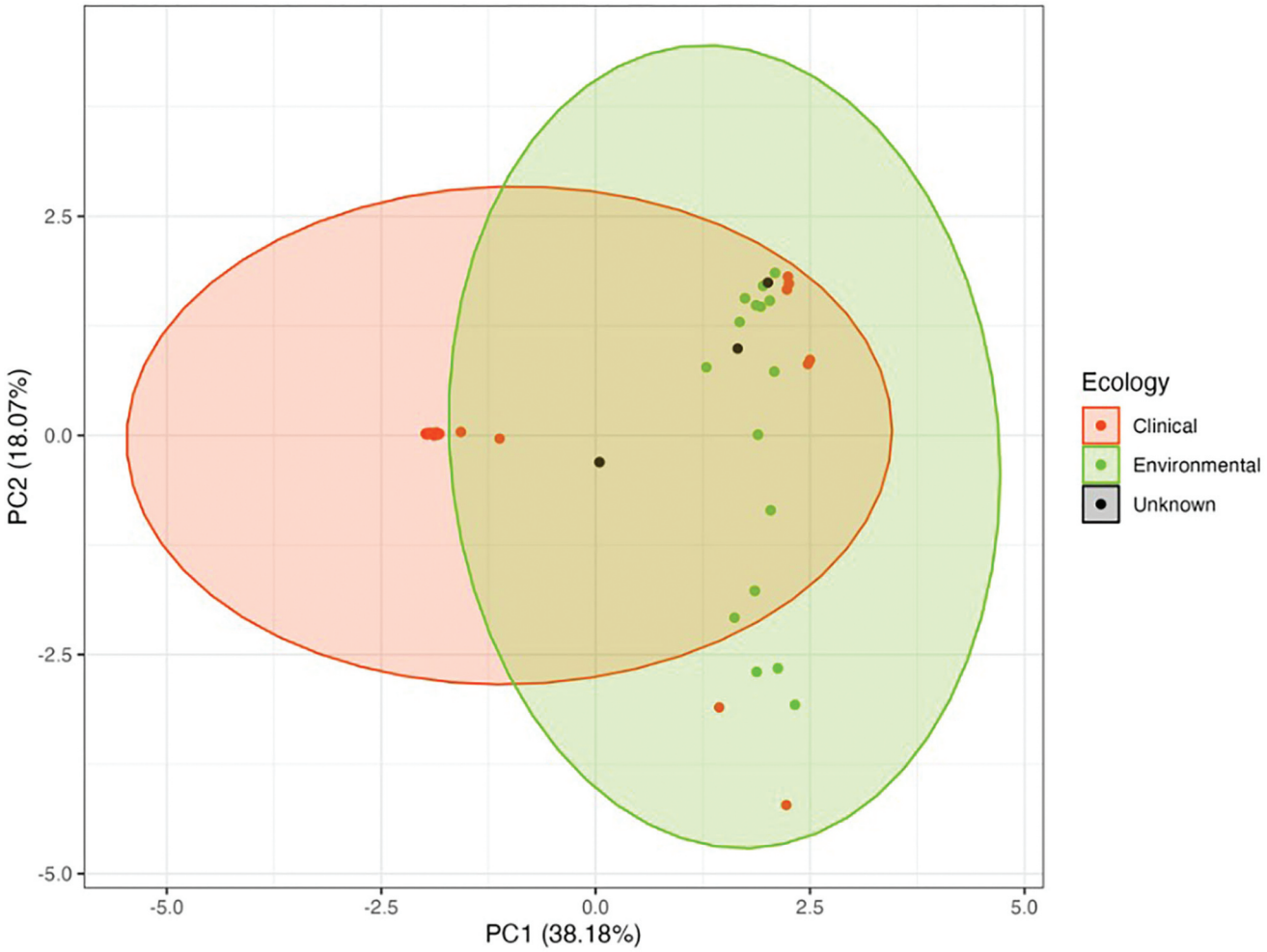

Figure 3. Similarity of *R. microsporus* data evaluated from whole genome single nucleotide polymorphism data. Principal component analysis (PCA) of the genomic diversity within *R. microsporus* using 6071 SNP markers. Axes indicate the total variance that is explained by the first two principal components. Isolation source is represented by clinical (red), environmental (green), and unknown (black), with 95% confidence ellipses for each group.

the high diversity found in environmental sources and a subset of more closely related isolates in clinical settings, providing further evidence of a clonal lineage (FIG. 3). Taken together, these results demonstrate the global ubiquity of *R. microsporus* and that a subset of isolates originating from the environment are isolated from clinical settings.

***Environmentally isolated* R. microspores *isolates exhibit more variable growth rates than their clinical counterparts.*—**We quantified radial mycelial growth rates of fungal colonies on 2% malt extract agar plates at 22 and 37 C to evaluate whether isolates from clinical and environmental settings differ in their growth rates at temperatures reflective of their isolation sources. We found that there was a significant difference in radial mycelial growth rates of all *R. microsporus* isolates grown at 37 C, regardless of isolation source (FIG. 5; ANOVA, P = 9.03e-08). Isolates grew 2.62 ± 0.99 mm/day at 22 C, whereas the average growth rate at 37 C was 4.46 ± 0.39 mm/day. However, when we compared growth rates between isolates by isolation source, we observed that environmentally derived isolates grew more variably and rapidly than clinical isolates at both temperatures, with a statistically significant increase at 22 C (FIG. 5; ANOVA, P = 0.022). We found that the interaction between isolation source and temperature was not significant (ANOVA, P = 0.23).

***Bacterial endosymbionts of* R. microspores *exhibit molecular diversity and irregular host association patterns.*—**To evaluate bacterial endosymbiont presence and host association in our newly sequenced *Rhizopus* isolates, we screened for bacteria using 16S

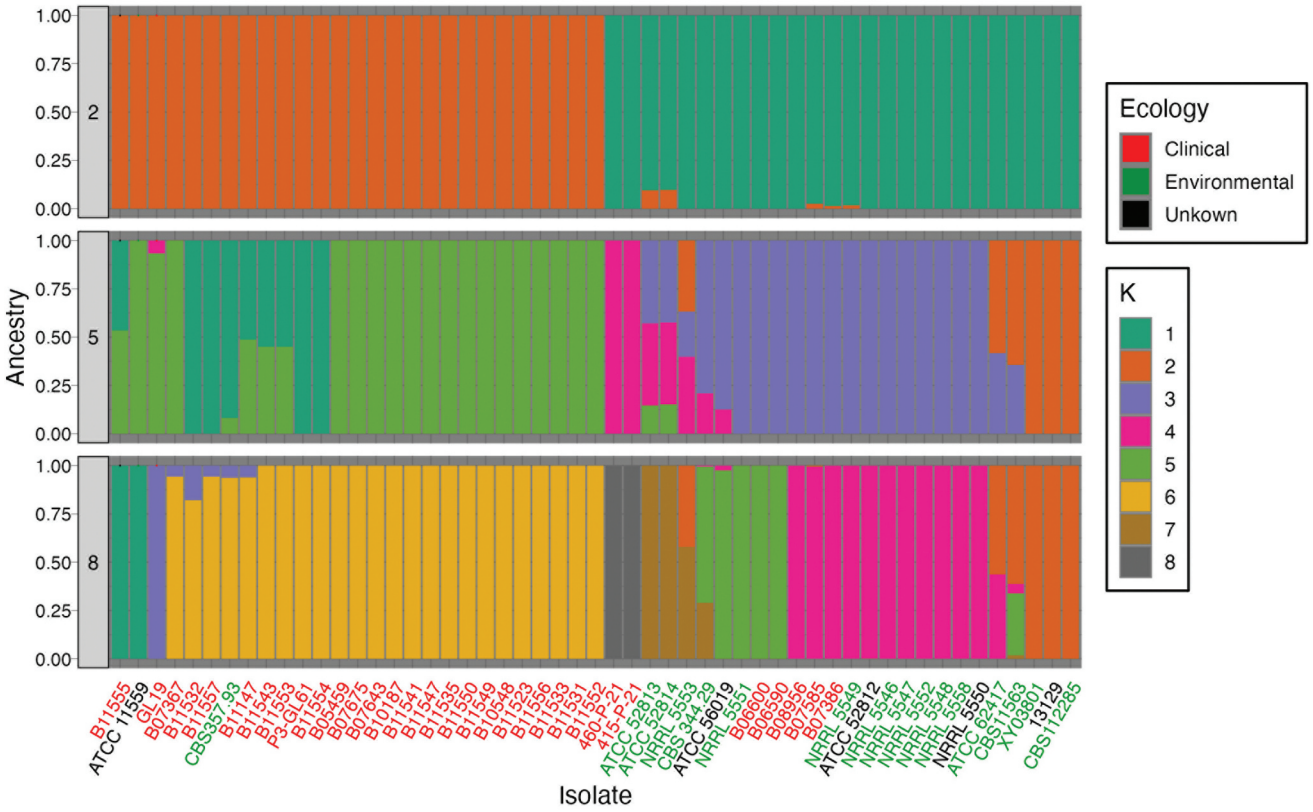

Figure 4. Population structure of *R. microsporus* isolates analyzed. ADMIXTURE bar plots displaying the genetic relationships of *R. microsporus* isolates using 6071 whole genome SNPs. Each bar plot represents the population structure for isolates given the optimal subpopulations K = 2, 5, and 8, respectively. Cross-validation error analysis for the ideal number of subpopulations resulted in K = 8. Isolation sources are indicated in the coloring of each isolate at the bottom of the figure: clinical (red), environmental (green), and unknown (black).

rDNA sequencing and analyses. We detected endosymbiotic bacterial DNA in 7 of 16 (~44%) of *R. microsporus* culture isolates (TABLE 1). During homology-based molecular analyses of the resulting 16S sequences, we observed that *R. microsporus* isolates ATCC 52811, ATCC 52814, CBS 112285, and NRRL 5546 hosted endosymbionts closely related to *Mycetohabitans endofungorum* isolate HKI 456 T. In contrast, isolates NRRL 5549, NRRL 5547, and ATCC 62417 hosted endobacteria closely related to *M. rhizoxinica* ATCC 27511. In summary, we observed using 16S rRNA sequence screening that less than half of *R. microsporus* harbored *Mycetohabitans* spp. endosymbionts related to *M. rhizoxinica* and *M. endofungorum*.

***Whole genome sequencing and assembly sizes reveal genomic architecture variation in* Rhizopus microspores.**—We compared genome assembly sizes of clinical and environmental *R. microsporus* isolates using new and publicly available sequence data. Genome sizes for the five newly sequenced *R. microsporus* isolates ranged from 27.8 to 29.1 Mb (TABLE 1). The remaining *R. microsporus* whole genome short-read assemblies were between 23.5 and 49.8 Mb (TABLE 1). The assembly sizes for the additional four *R. arrhizus* isolates obtained from publicly available, whole genome short reads were between 36.7 and 42.0 Mb (TABLE 1). To evaluate the accuracy of our genome size estimates, we used Nanopore to resequence a subset of *R. microsporus* isolates: NRRL 5546, ATCC 52814, and ATCC 62417. Genome assemblies based on Nanopore long reads produced assemblies with sizes from 27.7 Mb to 59.9 Mb, an increase of 15.0–17.3 Mb in genome assembly size compared with the assemblies derived only from Illumina data (TABLE 1). To evaluate whether the changes in genome size were attributable to increased repetitive content, especially in isolates whose assembly sizes increased significantly, we annotated transposable elements (TEs) using Earl Grey (Baril et al. 2024). We found that the relative proportion of each genome attributable to repetitive DNA, including TEs, was as follows: ATCC 62417, 13.94%; ATCC 52814, 20.62%; and 5546, 12.90% (SUPPLEMENTARY FIG. 1).

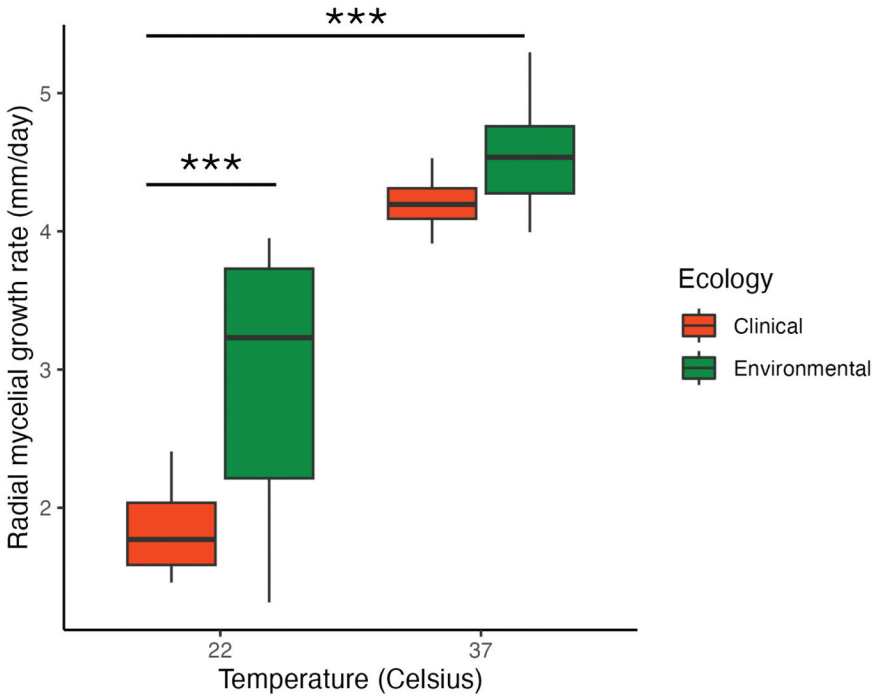

Figure 5. Radial growth rate of *R. microsporus* isolates by temperature and isolation source. Box plot measuring the radial mycelial growth rates (mm/day) of *R. microsporus*. Cultures were grown on 2% malt extract agar at 22 or 37 C. Isolation source is represented by clinical (red) and environmental (green) samples. Stars indicate statistical significance between treatments and isolation sources within treatments that are less than $P < 0.05$.

DISCUSSION

We used population and phylogenomic approaches to evaluate the evolutionary history and relatedness of *Rhizopus microsporus* isolates, leveraging new and existing genome sequence data from a total of 61 isolates, including 52 *R. microsporus*. We found that for isolates with known isolation sources, two clades are supported: one environmental clade with substantially more molecular diversity and one clinical clade derived from the environment (FIGS. 2–5). The clinical clade includes a clonal subpopulation from Argentina, whereas the environmental clade includes isolates from Africa, North America, South America, Asia, and Europe. In addition, we found evidence for active endosymbionts only in the environmental clade (TABLE 1), and all these isolates harbored endobacterial symbionts related to the genus *Mycetohabitans*. It is important to acknowledge that the geographic sampling of these species was not evenly distributed and that clinical isolates were overrepresented in our data set, likely due to an increased focus on mucormycosis given recent events and this emerging pathogen. In addition, we do not have historical culturing method data, including antibiotic treatment, for all isolates. However, similar studies have found between 15% and 57% Burkholderiaceae-related endobacteria (BRE) presence in Mucoromycota isolates (Lackner et al. 2009; Okrasińska et al. 2021). These data indicate that soil- and plant-associated environments are a diversity reservoir for *R. microsporus* and that a subset of these fungal species infect humans in clinical settings. In concurrence with our findings, the original paper that described the Argentinian isolates found that isolates were separated by between 60.0 and 912.0 bp with a mean difference of 430 SNPs between isolates, and they concluded that these clonal isolates were transmitted indirectly from a common source (Bowers et al. 2020).

To assess features that potentially differentiate clinical and environmental isolates, we evaluated endosymbiont presence and radial growth rate by temperature. We found that only isolates from environmental settings harbored endosymbionts and that endosymbionts were present in less than half (~44%) of the total isolates evaluated. We also observed that all endosymbionts belonged to species of *Mycetohabitans* based on analyses of 16S sequences. Although this is concurrent with recent reports on endosymbiont abundance (Dolatabadi et al. 2014; Okrasińska et al. 2021; Uehling et al. 2023), we lack culture metadata on many isolates included in this study and therefore endosymbiont abundance may be higher than these estimates. Our radial growth assays indicated that all *R. microsporus* isolates grew significantly faster at 37 C compared with 22 C and that environmental isolates

grew significantly faster than clinical isolates (FIG. 5). This suggests that in addition to the previous observation that clinical isolates grow at 37 C (Han and Nout 2000; Dolatabadi et al. 2014), clinical isolates may be selected for more restricted growth patterns than their environmental counterparts. Further, the variable and more rapid growth of environmental isolates may be underpinned by the molecular diversity observed in this study, which may enable insights into novel traits that facilitate virulence in humans. Overall, these results suggest that *R. microsporus* and *R. arrhizus* are well-supported species and that some isolates in public culture and sequence databases are potentially misannotated and can be curated using comparative analyses of whole genome data. In particular, isolate ATCC 56028 is currently accessioned in GenBank and the ATCC culture collection as *R. microsporus* but allies with the *R. arrhizus* in our analyses (FIGS. 2 and 3), and it is listed as both species in published literature. Gaining a more accurate understanding of fungal diversity and relatedness in this group has large potential implications for physiological and genetic studies assumed to have focused at the intraspecific level and may shift currently accepted dogmas in these fields. It is also important to note, given the recent COVID-19–related Black fungus outbreak, that Indian isolates are underrepresented in this study and were not publicly available at the time of analyses. We found that isolate 415-P-21 from India grouped with environmental isolates in our analyses but cannot draw firm conclusions about its origin or physiology without analyzing data from other isolates in this region.

We observed a high level of variation in genome assembly size in *R. microsporus*, ranging from 24.4 to 49.8 Mb, but there were no clear patterns within or between clinical and environmental isolates (FIGS. 2 and 3, TABLE 1). The majority of isolates are approximately 23.0–30.0 Mb, whereas some are 36.0–43.0 Mb, with assemblies up to 49 Mb when including Nanopore sequencing data. Previous studies have suggested a whole genome duplication event in the common ancestor of *R. microsporus* and the closely related species *R. arrhizus* (Ma et al. 2009; Gryganskyi et al. 2018). Our comparison of genome assembly size using both Illumina- and Nanopore-derived data further indicates that complex genomic architectures in *R. microsporus* may be the rule instead of the exception. For example, resequencing isolates ATCC 52814 and ATCC 62417 with Nanopore technologies increased genome assembly sizes by 15.0 and 17.3 Mb, respectively (TABLE 1). On the other hand, in isolate NRRL 5546, the assembly from Nanopore data (24.9 Mb) decreased by 2.8 Mb from the Illumina estimate (27.7 Mb). These differences in assembly length are likely attributed to the long reads spanning repetitive genomic regions (Pollard et al. 2018). On the other hand, aneuploidy, polyploidy, heterokaryosis, and bacterial endosymbionts could be responsible for assembly quality and size variation (Naranjo-Ortiz et al. 2022). To begin teasing out these contributing factors, we annotated TEs in our new Nanopore genome assemblies. We found that 12.91–20.62% of each genome was TEs (SUPPLEMENTARY FIG. 1), suggesting that in addition to previously observed whole genome duplication and high TE content, other processes have contributed to the very large genome assemblies in some isolates. We note that although ATCC 62417 had the largest genome of the three isolates sequenced by Nanopore technology, it contained a similar genomic proportion of TEs to its smaller conspecific isolates. These data indicate that long-read sequencing increases the quality of Mucoromycota genome assemblies and enables novel insights into complexities of aberrant genomic architectures, including duplicated and repetitive regions that were not previously detectable when studying genomes assembled from short-read sequencing technologies. Investigating which genes or regions are duplicated in *R. microsporus* genomes and whether these play a functional role will be a necessary future focus for the field. Together these data and analyses build a foundation for further genomic and molecular mechanistic studies.

In summary, we sequenced the genomes of six *R. microsporus* isolates and combined these with 55 whole genome sequences available on NCBI SRA and GenBank to assess relationships between clinical and environmental *R. microsporus* (TABLE 1). Our study is the largest data analysis for *Rhizopus microsporus* to date (Gryganskyi et al. 2018; Bowers et al. 2020; Nguyen et al. 2020) and is the first to connect environmental diversity with clinical associations. We found that there is a clinical subpopulation of isolates that are derived from environmental sources and are generally less diverse and have fewer endobacterial associations. We also observed that the environmental diversity reservoir is more physiologically diverse than clinical isolates and that genomic architecture is variable across *R. microsporus* regardless of the isolation source. Together these results suggest that environmental *R. microsporus* isolates are a diversity reservoir, including genetic, physiological, and symbiotic diversity that may enable variance in the subset of isolates that move on to cause infections in clinical settings. Although thermotolerance and endosymbiont-derived functional traits may partially contribute to virulence in human pathogenic *Rhizopus* species, there is much to be learned about their biology. Gaining a fundamental

understanding of *R. microsporus* genomic architecture, endosymbiont status, and interaction biology in environmental populations will serve as a foundation for future studies of virulence in these fungi.

DISCLOSURE STATEMENT

No potential conflict of interest was reported by the author(s).

DATA AVAILABILITY STATEMENT

Alignments are available in the supplementary files S1 and S2.

FUNDING

This work was supported by,Division of Environmental Biology, Division of Integrative Organismal Systems NSF 2202410 to J.K.U., NSF 2030338 to J.K.U., T.E.P., and R.A., and BBSRC BB/W002760/1 to E.R.B. and J.S.K.

ORCID

Jessie K. Uehling http://orcid.org/0000-0002-8705-5893

LITERATURE CITED

Alexander DH, Novembre J, Lange K. 2009. Fast model-based estimation of ancestry in unrelated individuals. Genome Res. 19(9):1655–1664. https://doi.org/10.1101/gr.094052.109

Amses K, Davis W, James T. 2019. SCGid: a consensus approach to contig filtering and genome prediction from single-cell sequencing libraries of uncultured eukaryotes. Bioinformatics. 36(7):1994–2000. https://doi.org/10.1093/bioinformatics/btz866

Antoniadou A. 2009. Outbreaks of zygomycosis in hospitals. Clin Microbiol Infect. 15(Suppl 5):55–59. https://doi.org/10.1111/j.1469-0691.2009.02982.x

Baker G, Smith JJ, Cowan DA. 2003. Review and re-analysis of domain-specific 16s primers. J Microbiol Methods. 55 (3):541–555. https://doi.org/10.1016/j.mimet.2003.08.009

Bankevich A et al. 2012. SPAdes: a new genome assembly algorithm and its applications to single-cell sequencing. J Comput Biol. 19(5):455–477. https://doi.org/10.1089/cmb.2012.0021

Baril T, Galbraith J, Hayward A. 2024. Earl grey: a fully automated user-friendly transposable element annotation and analysis pipeline. Mol Biol Evol. 41. https://doi.org/10.1093/molbev/msae068

Bowers JR et al. 2020. Rhizopus microsporus infections associated with surgical procedures, Argentina, 2006-2014. Emerg Infect Dis. 26:937–944. https://doi.org/10.3201/eid2605.191045

Cabrera-Rangel JF et al. 2022. Symbiotic and toxinogenic Rhizopus spp. isolated from soils of different papaya producing regions in Mexico. Front Fungal Biol. 3:893700. https://doi.org/10.3389/ffunb.2022.893700

Capella-Gutiérrez S, Silla-Martínez JM, Gabaldón T. 2009. Trimal: a tool for automated alignment trimming in large-scale phylogenetic analyses. Bioinformatics. 25 (15):1972–1973. https://doi.org/10.1093/bioinformatics/btp348

Carpenter SCD et al. 2024. Prevalence and diversity of TAL effector-like proteins in fungal endosymbiotic Mycetohabitans spp. Microb Genom. 10(6). https://doi.org/10.1099/mgen.0.001261

Chen S, Zhou Y, Chen Y, Gu J. 2018. fastp: an ultra-fast all-in-one FASTQ preprocessor. Bioinformatics. 34(17):i884–i890. https://doi.org/10.1093/bioinformatics/bty560

Cheng VCC et al. 2009. Outbreak of intestinal infection due to Rhizopus microsporus. J Clin Microbiol. 47(9):2834–2843. https://doi.org/10.1128/JCM.00908-09

Corzo-León DE, Chora-Hernández LD, Rodríguez-Zulueta AP, Walsh TJ. 2018. Diabetes mellitus as the major risk factor for mucormycosis in Mexico: epidemiology, diagnosis, and outcomes of reported cases. Med Mycol. 56 (1):29–43. https://doi.org/10.1093/mmy/myx017

Danecek P et al. 2021. Twelve years of SAMtools and BCFtools. Gigascience. 10(2):giab008. https://doi.org/10.1093/gigascience/giab008

De Coster W, D'Hert S, Schultz DT, Cruts M, Van Broeckhoven C. 2018. Nanopack: visualizing and processing long-read sequencing data. Bioinformatics (Oxford, England). 34:2666–2669. https://doi.org/10.1093/bioinformatics/bty149

Dolatabadi S, Walther G, Gerrits van den Ende AHG, de Hoog GS. 2014. Diversity and delimitation of Rhizopus microsporus. Fungal Divers. 64:145–163. https://doi.org/10.1007/s13225-013-0229-6

Eddy SR. 1996. Hidden Markov models. Curr Opin Struct Biol. 6:361–365. https://doi.org/10.1016/S0959-440X(96)80056-X

Eddy SR. 2011. Accelerated profile HMM searches. PLOS Comput Biol. 7:e1002195. https://doi.org/10.1371/journal.pcbi.1002195

Gryganskyi AP et al. 2018. Phylogenetic and phylogenomic definition of Rhizopus species. G3. 8:2007–2018. https://doi.org/10.1534/g3.118.200235

Han B-Z, Nout RMJ. 2000. Effects of temperature, water activity and gas atmosphere on mycelial growth of tempe fungi Rhizopus microsporus var. microsporus and R. microsporus var. oligosporus. World J Microbiol Biotechnol. 16(8–9):853–858. https://doi.org/10.1023/A:1008974621698

Ibrahim AS, Spellberg B, Walsh TJ, Kontoyiannis DP. 2012. Pathogenesis of mucormycosis. Clin Infect Dis. 54(Suppl 1):S16–22. https://doi.org/10.1093/cid/cir865

Itabangi H et al. 2022. A bacterial endosymbiont of the fungus Rhizopus microsporus drives phagocyte evasion and opportunistic virulence. Curr Biol. 32:1115–1130.e6. https://doi.org/10.1016/j.cub.2022.01.028

Jeong W et al. 2019. The epidemiology and clinical manifestations of mucormycosis: a systematic review and meta-analysis of case reports. Clin Microbiol Infect. 25:26–34. https://doi.org/10.1016/j.cmi.2018.07.011

Jombart T. 2008. Adegenet: a R package for the multivariate analysis of genetic markers. Bioinformatics. 24:1403–1405. https://doi.org/10.1093/bioinformatics/btn129

Kaerger K et al. 2015. Adaptation to thermotolerance in Rhizopus coincides with virulence as revealed by avian and invertebrate infection models, phylogeny, physiological and metabolic flexibility. Virulence. 6:395–403. https://doi.org/10.1080/21505594.2015.1029219

Kalyaanamoorthy S, Minh BQ, Wong TKF, von Haeseler A, Jermiin LS. 2017. ModelFinder: fast model selection for accurate phylogenetic estimates. Nat Methods. 14:587–589. https://doi.org/10.1038/nmeth.4285

Kang DD et al. 2019. Metabat 2: an adaptive binning algorithm for robust and efficient genome reconstruction from metagenome assemblies. PeerJ. 7:e7359. https://doi.org/10.7717/peerj.7359

Kolmogorov M, Yuan J, Lin Y, Pevzner PA. 2019. Assembly of long, error-prone reads using repeat graphs. Nat Biotechnol. 37(5):540–546. https://doi.org/10.1038/s41587-019-0072-8

Kontoyiannis DP, Lewis RE. 2011. How I treat mucormycosis. Blood. 118(5):1216–1224. https://doi.org/10.1182/blood-2011-03-316430

Lackner G et al. 2009. Global distribution and evolution of a toxinogenic Burkholderia-Rhizopus symbiosis. App Environ Microbiol. 75:2982–2986. https://doi.org/10.1128/AEM.01765-08

Lackner G, Hertweck C. 2011. Impact of endofungal bacteria on infection biology, food safety, and drug development. PLOS Pathogens. 7:e1002096. https://doi.org/10.1371/journal.ppat.1002096

Lackner G, Moebius N, Partida-Martinez LP, Boland S, Hertweck C. 2011. Evolution of an endofungal lifestyle: deductions from the Burkholderia rhizoxinica genome. BMC Genomics. 12:210.

Li H. 2011. A statistical framework for SNP calling, mutation discovery, association mapping and population genetical parameter estimation from sequencing data. Bioinformatics. 27(21):2987–2993. https://doi.org/10.1093/bioinformatics/btr509

Li H. 2013. Aligning sequence reads, clone sequences and assembly contigs with BWA-MEM. figshare. axriv. https://arxiv.org/abs/1303.3997

Li H et al. 2009. The sequence alignment/map format and SAMtools. Bioinformatics. 25:2078–2079.

Ma L-J et al. 2009. Genomic analysis of the basal lineage fungus Rhizopus oryzae reveals a whole-genome duplication. PLOS Genetics. 5(7):e1000549. https://doi.org/10.1371/journal.pgen.1000549

Millon L et al. 2013. Quantitative polymerase chain reaction detection of circulating DNA in serum for early diagnosis of mucormycosis in immunocompromised patients. Clin Infect Dis. 56(10):e95–e101. https://doi.org/10.1093/cid/cit094

Minh BQ et al. 2020. Iq-tree 2: new models and efficient methods for phylogenetic inference in the genomic era. Mol Biol Evol. 37(5):1530–1534. https://doi.org/10.1093/molbev/msaa015

Naranjo-Ortiz MA, Molina M, Fuentes D, Mixão V, Gabaldón T. 2022. Karyon: a computational framework for the diagnosis of hybrids, aneuploids, and other non-standard architectures in genome assemblies. GigaScience. 11. https://doi.org/10.1093/gigascience/giac088

Nguyen L-T, Schmidt HA, von Haeseler A, Minh BQ. 2015. Iq-tree: a fast and effective stochastic algorithm for estimating maximum-likelihood phylogenies. Mol Biol Evol. 32(1):268–274. https://doi.org/10.1093/molbev/msu300

Nguyen MH et al. 2020. Genetic diversity of clinical and environmental Mucorales isolates obtained from an investigation of mucormycosis cases among solid organ transplant recipients. Microbial Genomics. 6(12). https://doi.org/10.1099/mgen.0.000473

Okrasińska A et al. 2021. New endohyphal relationships between Mucoromycota and Burkholderiaceae representatives. App Environ Microbiol. 87(7). https://doi.org/10.1128/AEM.02707-20

Palmer JM, Stajich J. 2020. Funannotate Version.8.1: Eukaryotic genome annotation.

Pandey M et al. 2018. Emerging Rhizopus microsporus infections in India. J Clin Microbiol. 56(6). https://doi.org/10.1128/JCM.00433-18

Partida-Martinez LP et al. 2007. Burkholderia rhizoxinica sp. nov. and Burkholderia endofungorum sp. nov. bacterial endosymbionts of the plant-pathogenic fungus Rhizopus microsporus. Inter J Syst Evol Microbiol. 57(11):2583–2590. https://doi.org/10.1099/ijs.0.64660-0

Partida-Martinez LP, Hertweck C. 2005. Pathogenic fungus harbours endosymbiotic bacteria for toxin production. Nature. 437(7060):884–888. https://doi.org/10.1038/nature03997

Peixoto SC, Jorge JA, Terenzi HF, de Polizeli MLTM. 2003. Rhizopus microsporus var. rhizopodiformis: a thermotolerant fungus with potential for production of thermostable amylases. Inter Microbiol. 6:269–273. https://doi.org/10.1007/s10123-003-0140-1

Pollard MO, Gurdasani D, Mentzer AJ, Porter T, Sandhu MS. 2018. Long reads: their purpose and place. Human Mol Genetics. 27:R234–R241. https://doi.org/10.1093/hmg/ddy177

Prakash H et al. 2020. An aero mycological analysis of mucormycetes in indoor and outdoor environments of northern India. Med Mycol. 58(1):118–123. https://doi.org/10.1093/mmy/myz031

Prakash H, Chakrabarti A. 2019. Global epidemiology of mucormycosis. J Fungi (Basel, Switzerland). 5. https://doi.org/10.3390/jof5010026

Prakash H, Chakrabarti A. 2021. Epidemiology of mucormycosis in India. Microorganisms. 9(3):523. https://doi.org/10.3390/microorganisms9030523

Purcell S et al. 2007. Plink: a tool set for whole-genome association and population-based linkage analyses. Am J Human Genetics. 81:559–575. https://doi.org/10.1086/519795

Reysenbach AL, Giver LJ, Wickham GS, Pace NR. 1992. Differential amplification of rRNA genes by polymerase chain reaction. Appl Environ Microbiol. 58(10):3417–3418. https://doi.org/10.1128/aem.58.10.3417-3418.1992

Richter I et al. 2024. Deazaflavin metabolite produced by endosymbiotic bacteria controls fungal host reproduction. ISME J. 18(1):wrae074. https://doi.org/10.1093/ismejo/wrae074

Robinson AJ et al. 2021. Widespread bacterial diversity within the bacteriome of fungi. Communications Biol. 4(1):1168. https://doi.org/10.1038/s42003-021-02693-y

Schipper M, Stalpers J. 1984. Revision of the genus Rhizopus. Stud Mycol. 25:1–34.

Skiada A et al. 2018. Challenges in the diagnosis and treatment of mucormycosis. Med Mycol. 56(Suppl 1):93–101. https://doi.org/10.1093/mmy/myx101

Spellberg B, Walsh TJ, Kontoyiannis DP, Edwards JJ, Ibrahim AS. 2009. Recent advances in the management of mucormycosis: from bench to bedside. Clin Infect Dis. 48:1743–1751. https://doi.org/10.1086/599105

Uehling J et al. 2017. Comparative genomics of Mortierella elongata and its bacterial endosymbiont Mycoavidus cysteinexigens. Environ Microbiol. 19:2964–2983. https://doi.org/10.1111/1462-2920.13669

Uehling JK et al. 2023. Bacterial endosymbionts of mucoromycota fungi: diversity and function of their interactions. In: James T, editor. The mycota. Springer International Publishing. p 177–205.

Vaser R, Sović I, Nagarajan N, Šikić M. 2017. Fast and accurate de novo genome assembly from long uncorrected reads. Genome Res. 27(5):737–746. https://doi.org/10.1101/gr.214270.116

Verweij PE, Voss A, Donnelly JP, de Pauw BE, Meis JF. 1997. Wooden sticks as the source of a pseudoepidemic of infection with Rhizopus microsporus var. rhizopodiformis among immunocompromised patients. J Clin Microbiol. 35(9):2422–2423. https://doi.org/10.1128/jcm.35.9.2422-2423.1997

White TJ, Bruns T, Lee S, Taylor J. 1990. Amplification and direct sequencing of fungal ribosomal RNA genes for phylogenetics. In: Innis MA, Gelfand DH, Sninsky JJ, White TJ, editors. PCR protocols. Elsevier. p 315–322.

Zheng R-Y, Chen G, Huang H, Lt GS, Lt X-YL. 2007. A monograph of Rhizopus. Sydowia.